Required Buried α-Helical Structure in the Bilirubin UDP-Glucuronosyltransferase, UGT1A1, Contains a Nonreplaceable Phenylalanine

Marco Ciotti, Jeong W. Cho, John George,‡ and Ida S. Owens*

Human Genetics Branch, National Institute of Child Health and Human Development, National Institutes of Health, and Laboratory of Molecular Immunology, National Heart, Lung and Blood Institute, National Institutes of Health, Bethesda, Maryland 20892

Received April 2, 1998; Revised Manuscript Received May 21, 1998

ABSTRACT: A conserved hydrophobic region in the bilirubin-type UDP-glucuronosyltransferase isozyme was first uncovered as a consequence of a deleterious mutation in the UGT1A1 (HUG-Br1) isozyme of a Crigler−Najjar (CN) Type I patient. According to analysis by the RAOARGOS computer program, this hydrophobic region in UGT1A1 is located between residues 159−177 and defines a buried helix centered over position 169−172 with a positive factor of 1.22. Further analysis showed that the planar phenol-type UGT1A6 (HLUG P1) isoform, unlike the steroid-type UGT2B7 (UDPGTh2) isozyme, has a similar conserved hydrophobic region and that the positive factor for its buried helix is 1.14 compared to the threshold of 1.13 for such a structure. The analysis detected the typical membrane-insertion-signal sequence and a membrane-anchoring domain in each isoform. The different amino acid sequence patterns between positions 168−172 for the three types of isoforms and the deleterious mutations in this microregion (MRA) of UGT1A1 in CN-I patients are evidence of a critical and descriminating role for MRA. With the recombinant UGT1A1 enzyme and its mutants, P167G, F170del, F170L, F170I, F170V, F170A, F170Y, F170E, F171L, F171I, F171V, F171A, F171Y, or L175Q, expressed in COS-1 cells, bilirubin glucuronidating activity at both pH 6.4 and 7.6 demonstrated that Phe-170 is not replaceable, whereas Phe-171 can be replaced by Leu without any loss of activity. The less hydrophobic buried helix in the phenolic-type UGT1A6 has a Tyr/Leu at position 170/171; this isoform glucuronidated bilirubin at 1/10 the level of that by UGT1A1 with a Km (bilirubin) of 25 μM compared to that for UGT1A1 of 5.0 μM.

In humans, some 200−400 mg of heme-derived bilirubin IXa is produced daily from salvaged senescent red blood cells requiring detoxification to prevent hyperbilirubinemia and, potentially, neurotoxicity. At physiological pH, the dianionic bilirubin IXa internally hydrogen bonds creating a hydrophobic-behaving water-insoluble compound with special affinity for the phospholipids of the central nervous system. Thus, sustained severe hyperbilirubinemia will lead to lethal neurotoxicity (for review, see ref *1*). The endoplasmic reticulum bound bilirubin UDP-glucuronosyltransferase (transferase) covalently links glucuronic acid to either one or both of the propionic carboxyl groups of the derivative thereby producing either water-soluble bilirubin-IXaC8 monoglucuronide, bilirubin IXaC12 monoglucuronide, or bilirubin IXaC8C12 diglucuronide. Evidence from the genetically transmitted Crigler−Najjar (CN) Type-I disease characterized by the total impairment of bilirubin transferase activity (*2*) and the associated lethal neurotoxicity (*1*) indicates that this enzyme system is the only effective mechanism for the clearance of bilirubin from humans. Thus, bilirubin transferase, critical to bilirubin homeostasis, removes the large daily load generated by the heme oxygenase-biliverdin reductase system of the spleen.

The isolation and expression of two different human bilirubin transferase cDNA clones (*3*) allowed for the first critical characterization of the bilirubin isoform, UGT1A1 (HUG-Br1), and a less abundant and minor bilirubin isoform (UGT1A4, HUG-Br2). These studies demonstrated for the first time that either isoform expressed in COS-1 cells could generate the three bilirubin glucuronides. Furthermore, the cDNA clones were used as probes to isolate and describe the novel genetic locus, *UGT1A* (*4*, *5*), which encodes the bilirubin and the phenol isoforms. Each of the isoforms encoded at this locus shares a common carboxyl terminus (*4*).

Although some 25−30 deleterious mutations at the *UGT1A1* gene have been shown to cause CN Type I disease (*2*, *6*, *7*), certain missense mutations have been invaluable in delineating essential structures (*8*, *9*) in the bilirubin isoform.

Because bilirubin transferase-replacement includes primarily the invasive liver transplantation strategy and, predictably, gene therapy in the future, it is necessary to understand the essential elements of catalysis by the wild-type transferase in order to understand how to adapt and enhance the activity of certain of the mutant versions found in the population. In this study, we have focused on the disruption of a unique and essential hydrophobic microregion, designated MRA, in the UGT1A1 bilirubin isoform and the structure−function relationship of a conserved diphenylalanine in this region of bilirubin-type isoforms. Further, the effects of deleterious mutations in this region found in Crigler−Najjar Type I patients are compared.

* Corresponding author. National Institutes of Health, Building 10, Room 9S-242, Bethesda, MD 20892-1830. Phone: 301-496-6091.

S0006-2960(98)00747-8 CCC: $15.00
Published on Web 07/16/1998

MATERIALS AND METHODS

Materials. The sources of reagents used to carry out recombinant DNA techniques are already described (*8*). The TA vector was obtained from Invitrogen (San Diego, CA). The sources of materials for (a) the transfection of plasmid DNA into COS-1 cells, (b) the radiolabeling and immunoprecipitation of the in vitro expressed bilirubin transferase protein, and (c) the bilirubin glucuronidation assay are detailed in previous reports (*8, 10*).

History of the Crigler−Najjar Patient. After birth, the serum unconjugated bilirubin of the patient, LC, reached 470 μM before phototherapy treatment was begun that maintained the concentrations between 90 and 130 μM; normal levels range between 8.6 and 16.2 μM. At 3 weeks and at 6 months of age, the hyperbilirubinemia did not respond to phenobarbital treatment.

Isolation of Genomic DNA. Genomic DNA was isolated from blood samples of the CN-I individual (proband) and the parents as already detailed (*2*).

Polymerase Chain Reaction, Subcloning, and Sequencing of PCR Products. Sequence analysis showed that the CN-I patient, LC, contained a missense mutation within MRA. Hence, we included the characterization of that protein in this study. Exon 1 and the 4 common ones of the *UGT1A1* gene of the patient were amplified by polymerase chain reaction (PCR) and sequenced as described (*2*). A point mutation (CTG to CAG) converting codon 175 for Leu to Gln was uncovered in one allele (2/10 subclones) of exon 1 of the *UGT1A1* gene of the patient. The allele is predicted to produce a full-length mutant protein with the substitution L175Q. Sequencing the appropriate genomic DNA subclones (2/10) revealed that the mother is heterozygous for this missense mutation. Also, nucleotide G was deleted (2/5 subclones) at codon 325 (nt 973) in the common exon 2 on the other allele of patient LC; the deletion is predicted to generate a premature stop codon at 365. The genome of the father is also missing a G at nucleotide 973 (2/6 subclones) of the *UGT1A1* gene. Genotypically, LC is a compound heterozygote, L175Q/973 del G. No nucleotide sequence data are shown.

Construction of Altered pUGT1A1 Expression Units. All of the MRA mutants were constructed in the pSVL-based UGT1A1 (HUG-Br1) unit which was previously described (*3*). The point mutations were introduced at codon 167, 170, 171, or 175 of the UGT1A1cDNA. The mutated codons are designated as follows: P167G, F170del, F170L, F170I, F170V, F170A, F170Y, F170E, F171L, F171I, F171V, F171A, F171Y, or L175Q. F170del and L175Q represent the *UGT1A1*13* and *UGT1A1*12* allele, respectively, uncovered in different CN-I individuals by Ritter et al. (*8*) and by Seppen et al. (*11*). The alleles were recently named following the formulation of a nomenclature strategy for the isozymes of the UDP-glucuronosyltransferase superfamily (*7*). Two independent PCR reactions were carried out for each of the above mutant codons, except for L175Q, using the following primers: P167G, sense (5′-CTGTCTCTGGGTACTGTATTCT-3′) and antisense(5′-AGAATACAGTACCCAGAGACAG-3′); F170L, sense (5′-CCCACTGTATTGTTCTTGC-3′) and antisense (5′-GCAAGAACAATACAGTGGGCAG-3′); F170I, sense (5′-CTGCCCACTGTAATCTTCTTG-3′) and antisense (5′-CAAGAAGATTACAGTGGGCAG-3′); F170V, sense (5′-CTGCCCACTGTAGTCTTCTTGC-3′); and antisense 5′-GCAAGAAGACTACAGTGGGCAG-3′; F170A, sense (5′-CTGCCCACTGTAGCCTTCTTG-3′) and antisense (5′-CAAGAAGGCTACAGTGGGCAG-3′); F170Y, sense (5′-CTGCCCACTGTATATTTCTTGC-3′) and antisense (5′-GCAAGAAATATACAGTGGGCAG-3′); F170E, sense (5′-CTGCCCACTGTAGAGTTCTTG-3′) and antisense (5′-CAAGAACTCTACAGTGGGCAG-3′); F171L, sense (5′-CCCACTGTATTCTTGTTGCAT-3′) and antisense (5′-ATGCAACAAGAATACAGTGGG-3′); F171I, sense (5′-CTGCCCACTGTATTCATCTTG-3′) and antisense (5′-CAAGATGAATACAGTGGGCAG-3′); F171V, sense (5′-CCCACTGTATTCGTCTTGCATGCA-3′) and antisense (5′-TGCATGCAAGACGAATACAGTGGG-3′); F171A, sense (5′-CCCACTGTATTCGCCTTGCATGCA-3′) and antisense (5′-TGCATGCAAGGCGAATACAGTGGG-3′); F171Y, sense (5′-CCCACTGTATTCTATTTGCATGCA-3′) and antisense (5′-TGCATGCAAATAGAATACAGTGGG-3′.

The outside primer set for all mutations was OP170, sense (5′-CAGGGCGGACGCCCACTTGT-3′), and PXAS6, antisense (5′-TAAACACCATGGGAACC-3′). Each sense primer used with the antisense PXAS6 generated a 652 bp fragment, whereas the antisense primer used with the sense primer OP170 generated a 484 bp fragment. The interchanged hybridizing fragment generated by combining the 652 and 484 bp PCR products was used as a primer in a reaction with the primer set, OP170 and PXAS6. The reaction generated a 1136 bp fragment containing the mutation of interest. The fragment was digested with *Apa*I and *Bst*EII; the resulting 1020 bp fragment was ligated into the *ApaI/Bst*EII-digested wild-type expression unit, pSVL-UGT1A1. The replaced fragment contained each of the mutations. The replaced segment, including the ligation sites, was sequenced to ensure that no other changes occurred in the reading frame.

The L175Q mutant of UGT1A1 was constructed by amplifying the exon 1 of *UGT1A1* of the CN-I patient with primer set PAG4 and PAG5 (*8*) to generate a 990 bp fragment which was subcloned into the TA vector. After digestion of the insert with *Apa*I and *Bsa*AI, the excised 512 bp fragment was ligated into *Apa*I/*Bsa*AI-digested pSVL-based UGT1A1. The L175Q allele was recently designated *UGT1A1*12* (*7*). The replaced segment and ligation sites were sequenced to ensure that no other changes occurred in the reading frame. The phenolic-type UGT1A6 expression unit was cloned as described (*10*).

Expression of the Units with the Wild-Type and Altered cDNA in COS-1 Cells and Immunocomplexing of Protein. COS-1 cells were plated in 100 mm dishes at 10^6 cells and grown to 90% confluency in 24 h in Dulbecco's Modified Eagle's Medium (DMEM) with Hepes buffer and 4% fetal calf serum (FCS); pUGT1A1 or each of its mutants was transfected into cells using DEAE-Dextran as the carrier as described (*8, 9*). In addition, the phenol-type UGT1A6 was expressed. The transferase isozymes were radiolabeled during the final 4 h of the incubation as previously described (*8, 12*). Goat anti-mouse UDP-glucuronosyltransferase IgG was added to the solubilized labeled cellular extract and processed for SDS−gel electrophoresis as described (*8, 12*); the dried gel was scanned on the Fuji Phosphorimager BAS 2000 and exposed to X-ray film for an autoradiograph. The

Table 1: Comparison of the Hydrophobicity in the Microregion A of Three Types of UDP-Glucuronosyltransferases[a]

Bilirubin-type	152			156					161							167		170				173	175				180		
UGT1A1 (HUG-Br1)	P	F	L	P	C	S	P	I	V	A	Q	Y	L	S	L	P	T	V	F	F	L	H	A	L	P	C	S	L	E
UGT1A3 (UGT1C)	P	V	N	L	C	A	A	V	L	A	K	Y	L	S	I	P	T	V	F	F	L	R	N	I	P	C	D	L	D
UGT1A4 (HUG-Br2)	P	V	N	L	C	G	A	V	L	A	K	Y	L	S	I	P	A	V	F	F	W	A	Y	I	P	C	D	L	D
UGT1A5 (UGT1E)	P	F	H	L	C	A	A	V	L	A	K	Y	L	S	I	P	A	V	F	F	L	R	N	I	P	C	D	L	D
UGT1A1 (Rat Bil UDPGT)	P	V	F	P	C	G	A	L	L	A	K	Y	L	Q	I	P	A	V	F	F	L	R	S	V	P	C	G	I	D
Ugt1a1 (Mouse Bil UDPGT)	P	F	L	P	C	G	S	I	V	A	Q	Y	L	T	V	P	T	V	Y	F	L	N	K	L	P	C	S	L	D
UGT1A04 (Rabbit UGT1-4)	P	L	D	L	C	G	A	L	L	A	K	Y	L	S	V	P	S	V	F	L	L	R	F	I	L	C	D	L	D
Simple Phenol-type																													
UGT1A6 (HLUG P1)	P	A	L	P	C	G	V	I	L	A	E	Y	L	G	L	P	S	V	Y	L	F	R	G	F	P	C	S	L	E
UGT1A6 (Rat Phenol UDPGT)	P	A	M	P	C	G	V	I	L	A	E	Y	L	K	L	P	S	I	F	L	F	R	G	F	P	C	S	L	E
Ugt1a6 (Mouse Phenol UDPGT)	P	F	D	V	C	G	L	I	V	A	K	Y	F	S	L	P	S	V	I	F	A	R	G	V	F	C	D	Y	L	E
UGT1A6 (Rabbit Phenol UDPGT)	P	A	L	P	C	G	V	I	L	A	E	Y	L	G	L	P	S	V	Y	L	F	R	G	F	P	C	S	L	E
Steroid-type																													
UGT2B7 (UDPGTh-2)	A	I	F	P	C	S	E	L	L	A	E	L	F	N	I	P	F	V	Y	S	L	S	F	S	P	G	Y	T	F	E
UGT2B15 (UDPGTh-3)	A	L	N	P	C	G	E	L	L	A	E	L	F	N	I	P	F	L	Y	S	L	R	F	S	V	G	Y	T	F	E
UGT2B1 (UDPGTr-1)	A	V	G	P	C	G	E	L	L	A	E	L	L	K	T	P	L	V	Y	S	L	R	F	C	P	G	Y	R	C	E
UGT2B2 (UDPGTr-4)	P	V	A	S	C	G	E	L	I	A	E	L	L	Q	I	P	F	L	Y	S	I	R	F	S	P	G	Y	Q	I	E
UGT2B14 (Rabbit)	A	I	G	P	C	G	E	L	L	A	E	L	L	K	I	P	F	V	Y	S	L	R	F	T	P	G	Y	T	M	E

[a] The microregion A (MRA) of the UGT1A1 protein was compared to that equivalent region in other bilirubin-type, simple-phenol type, and steroid-type isoforms from various species. UGT1A3, a human bilirubin-type, the minor bilirubin isoform, UGT1A4, (HUG-Br2), and bilirubin-forms from rat, mouse and rabbit are shown in lines 2−7. The mouse and rabbit bilirubin isoforms have not been expressed to verify bilirubin turnover. MRAs in human UGT1A6 (HLUG-P1), rat, mouse and rabbit simple-phenol isoforms are shown in lines 8−11. The hydrophobic residues 159−177 (dark shade) in UGTG1A1 and 152−175 in UGT1A6 define the buried helical structures; in both isoforms, the peak is centered over residue 169−172. The equivalent MRA in human UGT2B7 and human UGT2B15, rat UGT2B1, mouse UGT2B2, and rabbit UGT2B14 are shown in lines 12−16. The conserved Ser-168 in the phenol-type isoforms appears to be at position 171 in the steroid-type isoforms as indicated by the diagonal arrow and the shaded residues at the hydrophobic core of MRA. The detection of the buried helices are described in Figure 1 (arrow). Bold letters highlight conserved residues present in every form or where there are distinctions between types of isoforms. The amino acid position 152 is 150 for the rat bilirubin and phenol, 151 for UGT1A6, 153 for the UGT2B1, UGT2B2, UGT2B14, UGT2B15, UGT1A3, UGT1A4, and UGT1A5, and 154 for mouse bilirubin Ugt1a6 isoforms.

quantitation of the radiolabeled proteins was used to normalize for equal amounts of wild-type and mutant protein.

Assay for Bilirubin Glucuronidation. Cell homogenate containing expressed wild−type or mutant enzyme was used to determine bilirubin glucuronidation as described (*8*, *13*) with minor modifications (*9*, *10*). Since we have demonstrated (*8*) that the wild-type human bilirubin UGT1A1 glucuronidates bilirubin at a rate 2−3-fold higher at pH 6.4 than at pH 7.6, we carried out assays at both pH values for all versions of the isoform. Optimal conditions were as follows: 1.41 mM [^{14}C]UDP-glucuronic acid (1.41 mCi/mM), 5.0 mM $MgCl_2$, 16.6 mM saccharic acid, 1,4-lactone, and either 33 mM triethanolamine, pH 7.2, or 20 mM sodium phosphate, pH 6.4, in a total volume of 100 μL. After storage at −70 °C in PBS,[1] cell homogenates, spun at 10 000 rpm in a microfuge for 15 min to remove storage buffer, were resuspended in the reaction buffer containing $MgCl_2$ and saccharic acid 1,4-lactone; cellular protein was then treated with CHAPS (0.7 mg/mg of protein). Detergent-treated cell homogenate was added to the reaction vessel followed by [^{14}C]UDP-glucuronic acid. Bilirubin (10 mM) was dissolved in dimethyl sulfoxide, and 2.0 μL was added to the 98 μL reaction mixture and incubated at room temperature for 16 h. All subsequent manipulations and data analyses were carried out by TLC chromatography and scanned on the Ambis Radioanalytical Imaging System II for quantitation of product as already described (*12*). Mock transfected COS-1 cells contained no detectable bilirubin glucuronidating activity. Equal amount of specific protein used in each assay was determined as described above.

RESULTS

The discovery of an unusually hydrophobic and conserved sequence in the human UGT1A1 protein and other bilirubin-type isoforms [human: UGT1A4 (HUG-Br2) (*3*); UGT1A3 and UGT1A5 (*4*); rat UGT1A1 (*14*); mouse Ugt1a1 (*15*); and rabbit UGT1A04 (*16*)] was a consequence of a potentially lethal in-frame Phe-deletion mutation at amino acid residue 170 (F170del, *UGT1A1*13*) in a Crigler−Najjar type I patient; the surrounding sequence in the protein was designated microregion A (MRA) (*8*). Upon comparing the region in bilirubin isoforms to other classes of UDP-glucuronosyltransferase Table 1, it became evident that a characteristic and related sequence in this region identifies each of the three classes of transferases. The bilirubin- and phenol-type isoforms [human UGT1A6 (HLUG P1) (*17*); rat UGT1A6 (phenol UDPGT) (*18*); Ugt1a6 (mouse phenol UDPGT) (*15*); and Rabbit UGT1A6 (*19*)] contain an apparently highly hydrophobic sequence in the equivalent position from residue 167 to 172; this hydrophobicity is disrupted by Ser due to an apparent translocation at position 171 [Table 1 (diagonal arrow)] and an extra charged residue in the steroid isoforms.

Computer Analysis of UGT1A1, UGT1A6, and UGT2B7-(UDPGTh-2) Proteins Using the RAOARGOS Program. Because the evidence from the UGT1A1*13 mutant protein indicated that the hydrophobic region was essential for

[1] Abbreviations: CHAPS, (3-[3-cholamidopropyl]-dimethylammonio)-1-propane; PBS, phosphate buffer saline.

bilirubin glucuronidation, we used the RAOARGOS computer program (*20, 21*) to analyze for differences in this region among the three different transferase types: a bilirubin-type, a simple phenol-type, and a steroid-type as shown in Table 1. This program is designed to identify membrane-associated structures (*20*). With certain restrictions discussed,[2] the RAOARGOS program predicted, as shown in Figure 1, panels A and B (arrows), that a buried helix exists in both UGT1A1 and UGT1A6 between residues 159−172 and between 152 and 175 with a positive factor of 1.226 and 1.144, respectively. The core hydrophobicity is between 168 and 172 of the proteins. The lower limit for the positive factor is set at 1.13 to satisfy the designation buried helix. On the other hand, the steroid-type, UGT2B7 (*12*), is predicted to lack a buried helix in this region (Figure 1C, arrow). As defined by Mohana Rao and Argos in the footnote 2 and as shown in Table 1, both the bilirubin- and phenol-types meet the maximum of two charged amino acids in a buried helix containing between 16 and 35 residues while the steroid isoform contains three charged residues in this same region. Furthermore, the steroid-type isoform contains the α-helix-neutral Ser at position 171, the core of the hydrophobic region in the bilirubin- and phenol-types.

The program predicted that each of the three isoforms contains—like all isoforms studied to date—both a hydrophobic membrane-signal peptide and a membrane-anchoring domain at a position less than 30 residues from the amino terminus and between residues 495 and 514, respectively (Figure 1).

Expression of the Wild-Type and mutant Bilirubin UGT1A1 Isoforms. Because the four consecutive hydrophobic residues containing the diphenylalanine at position 170/171 in UGT1A1 have the greatest possibility of participating in an α-helix (*20*), of being buried (*22*), of being at the core of MRA, and because the Phe-170 deletion mutant caused the potentially

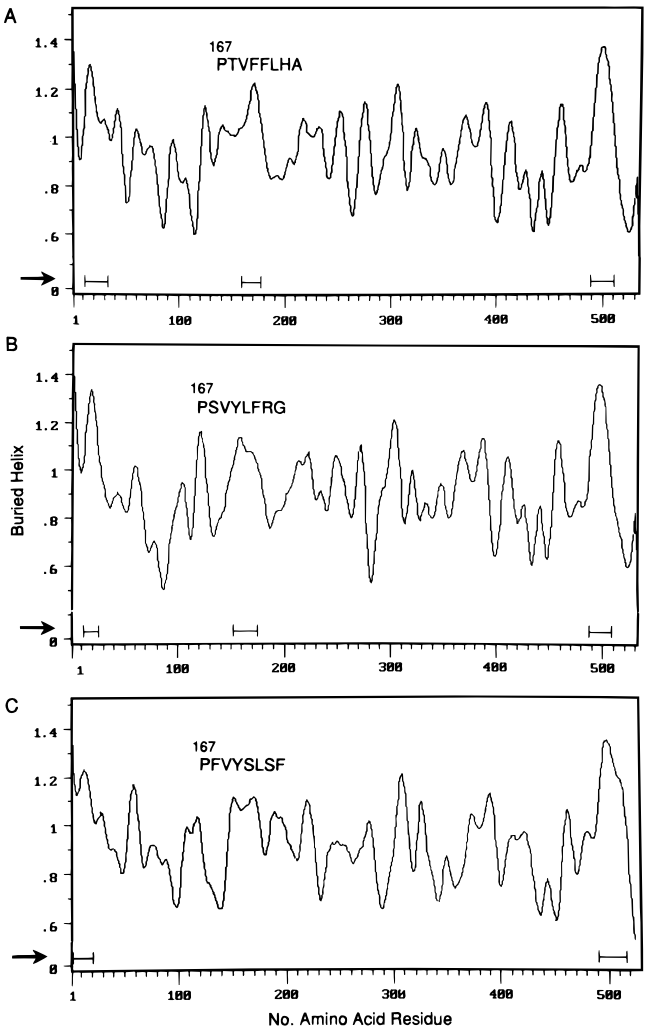

FIGURE 1: Plot of buried helices parameter versus amino acid sequence number for UGT1A1, UGT1A6, and UGT2B7. The buried-helix parameter for the bilirubin (UGT1A1), the human simple phenol (UGT1A6), and the steroid (UGT2B7) isoforms versus the amino acid sequence number is shown. A buried helix is shown (solid line) for all isoforms between position 1−30 and 480−519 for all isoforms. A third buried helical structure exists between 159 and 172 for UGT1A1 and between 152 and 175 for UGT1A6, respectively, with the peak over 169−172 in each case. The plots were obtained by using the RAOARGOS program which is designed to detect buried helix in membrane-bound proteins with criteria and restrictions described (*20, 21*).

lethal Crigler−Najjar type I disease, we have focused on this site to study the requirements for bilirubin glucuronidation. Mutants with conservative substitutions at both positions 170 and 171 with either Leu, Ile, Val, or Ala were studied to determine the critical nature of the hydrophobic residue at either position, and Tyr was substituted to compare hydrophobicity/aromaticity requirements. The effect of negatively charged Glu-170 was analyzed. Further, we studied the effect of L175Q, also seen in a Crigler−Najjar Type I individual, on hydrophobicity of the MRA and the evident total loss of in vivo bilirubin glucuronidation causing the severe hyperbilirubinemia in the patient.

We show in Figure 2 that the wild-type and each mutant cDNA unit expresses specific protein. In a previous study (*8*), the mass of both the UGT1A1 protein and its Phe-deletion mutant (UGT1A1*13) was shown to be 52 kDa. In this study, the mass of each of the mutant proteins is similar

[2] Briefly, the RAOARGOS program utilizes hydration potential, the free energy of transfer for a given residue type in a helix in aqueous medium to a helix in a nonpolar phase, polarity, bulk, and a turn conformational preference to predict sufficient α-helix to traverse or become buried within the membrane lipids. On the basis of the results of a survey of 49 integral membrane proteins generating 256 membrane-buried helices out of a total of 5632 predicted residues, the authors restricted the parameters which should be met in predicting α-helix with membrane association or membrane buried. (i) The minimum and maximum lengths of the predicted helices were set at 16 and 35 residues, respectively, to attain one helix that can span a typical membrane. (ii) Only those regions with positive prediction values that are at least 10 residues long and that are extendable by the inclusion of neighboring hydrophobic and weakly polar residues were considered to be possibly helical. (iii) Since lipid-associated helices have to interact with the interior of the membrane, it is expected to be devoid of charges. Charges in such a structure in some cases may be required. Topologically, the structure(s) could arrange in such a way that the charge(s) is not in contact with the lipid medium but is situated inside the cavities formed by the helical bundles. (iv) The analysis excludes positive peaks that possess more than three charges or more than five charged and strongly polar residues (Arg, Asn, Asp, Gln, Glu, Lys). A buried-helix parameter was developed from amino acid composition of consensus helical regions uncovered in the survey of families of cloned membrane-bound and integral-membrane proteins. The strong helix makers are Phe, Leu, Ile, Ala, Cys, Met, and Val, with Gly, Thr, Trp, Ser, and Tyr remaining neutral. Gly and Pro and charged residues (when present) tend to concentrate in the vicinity of the predicted helix midpoint. Histidine seems to cluster near the surface, but still inside the membrane bilayer. Aromatic side chains (His, Phe, Trp, and Tyr) tend to be spaced two or three residues apart enabling them to stack one above the other. Strongly polar residues, together with His and Tyr, have a high predicted potential for terminating membrane-buried helices.

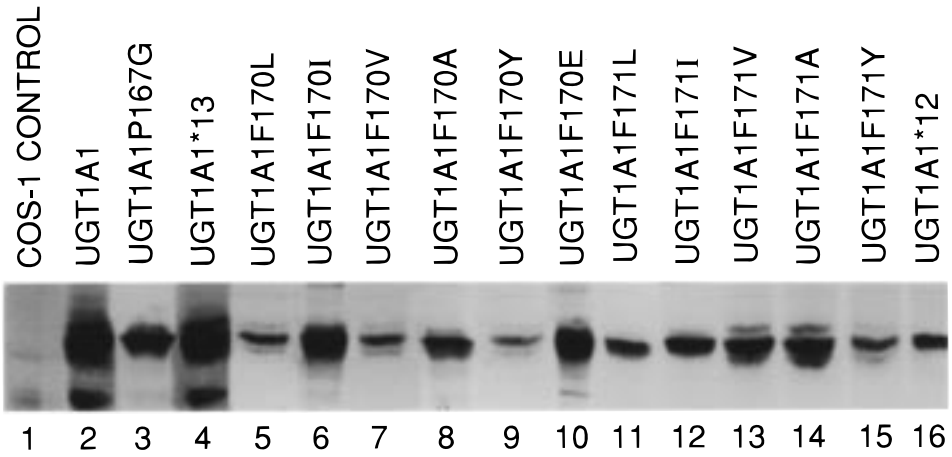

FIGURE 2: Immunocomplexes of pUGT1A1- or pUGT1A1-mutant transfected COS-1 cells following [^{35}S]methionine labeling. Cells were transfected with the pUGT1A1 or each of its mutants, radiolabeled with [^{35}S]methionine, solubilized, and immunocomplexed with goat anti-mouse UDP-glucuronosyltransferase immunoglobulin as described in the Materials and Methods (*12*). It has been shown (*8*) that the UGT1A1 (HUG-Br1) cDNA encodes a 52 kDa protein when expressed in COS-1 cell.

to the wild-type. Amounts of specific protein were normalized as described in the Materials and Methods in order to compare relative activities.

Structure−Function Relationship of Mutations at the Diphenylalanine in Position 170/171 of the Bilirubin UGT1A1 Isoform. As the Phe-170 deletion mutant (UGT1A1*13) (*8*) led to the discovery that the wild-type enzyme has 2−3-fold greater bilirubin glucuronidating activity at pH 6.4 relative to that at pH 7.6, we carried out all of our glucuronidation determinations at both pH values. It should be noted that control COS-1 cells had no detectable bilirubin transferase activity for bilirubin (Figure 3). Substitutions at the Phe-170 position showed that Leu allowed only 13 and 59% normal activity at pH 6.4 and 7.6, respectively (Figure 3). The incrementally less hydrophobic Val and Ala residues completely destroyed the pH 6.4 activity; only the Ala substitution further eroded the pH 7.6 activity reducing it to 10% normal. The bulky, but hydrophobic, Ile completely abolished activities. While the aromaticity of Tyr is comparable to that of Phe, its buried fraction (*22*) is far less; this substitution retained some 15 and 65% normal activity at pH 6.4 and 7.6, respectively. Negatively charged Glu at position 170, as might be predicted, supported no activity.

Phe at position 171 was less obligatory; replacement with the progressively more hydrophobic Ala, Val, and Leu showed 38, 51, and 100% normal activity at pH 6.4, respectively, and 44, 70, and 100% normal activity at pH 7.6%, respectively. Tyr-171 was 41% effective at pH 6.4 and was 100% at pH 7.6. The relative effectiveness of Tyr and Leu at the 170 and 171 positions indicates that both aromaticity and high hydrophobicity are important at 170 and that only high hydrophobicity, but not aromaticity, is critical at the 171 position. The total ineffectiveness of the hydrophobic α-helix-promoting Ile at both positions indicates that its more bulky and space-consuming properties are likely to disrupt tertiary structure abolishing all activity.

The mutant UGT1A1*12 protein, inherited by the at-risk hyperbilirubinemic CN-I patient with the substitution of a conserved hydrophobic residue at position 175 for Gln, revealed a total loss of activity at pH 6.4 with the retention of some 20% normal activity at pH 7.6. At each position, substitutions are more devastating to the pH 6.4 activity than that at pH 7.6.

Similarity of UGT1A6 (HLUGP1) and UGT1A1 in MRA. If we compare the character of the amino acid residues between 167 and 176 for the bilirubin- and the phenol-type isoforms in Table 1, the presence of a buried helix in this region of the human UGT1A6 in Figure 1, and the activities we obtained with conservative substitutions at the 170/171 positions of UGT1A1 shown in Figure 3, there is a suggestion that the UGT1A6 protein should be able to glucuronidate bilirubin if our assessment of this MRA is correct. The human UGT1A6 protein can glucuronidate bilirubin(data not shown), at least in vitro, at both pH values at 1/10 the level of that by UGT1A1and has a Km (bilirubin) of 25 uM compared to 5.0 uM for UGT1A1 (*8*).

DISCUSSION

Special features of the biochemically derived bilirubin IXα create its potential for toxicity and the difficulties associated with its detoxification. It is a water-insoluble, lipid-behaving internally hydrogen-bonded structure through its two carboxyl groups of the propionic acid substitutents and its two pyrrolenone rings. Since only the bilirubin IXα isomer—and not its IXβ, IXδ, and IX$_\gamma$ isomers—is capable of internally hydrogen bonding (*23*) and is the only one when administered (*24*) to animals that cannot be excreted without undergoing glucuronidation, it is likely that a hydrophobic interaction/binding of the heme derivative with the transferase occurs in order to dislodge the hydrogen bonds to allow for covalently linkage of glucuronic acid to the carboxyl group(s). The linkage creates a water-soluble and excretable bilirubin β-glucuronide. To avoid deposition in the central nervous system (*25*), bilirubin IXα is transported bound to albumin from spleen—its site of synthesis—to the liver via the blood (*26*) and is transported intrahepatocellularly bound to ligandin (*27*), presumably, to reach the site of glucuronidation in the lumen of the endoplasmic reticulum.

Evidence indicates that each of the two specific bilirubin-binding sites in albumin (reviewed in refs *26* and *28*) is composed of six subdomains with three 22 residue α-helices each connected and folded via pliable hinge regions. The helices include the aromatic residues Phe and Tyr satisfying

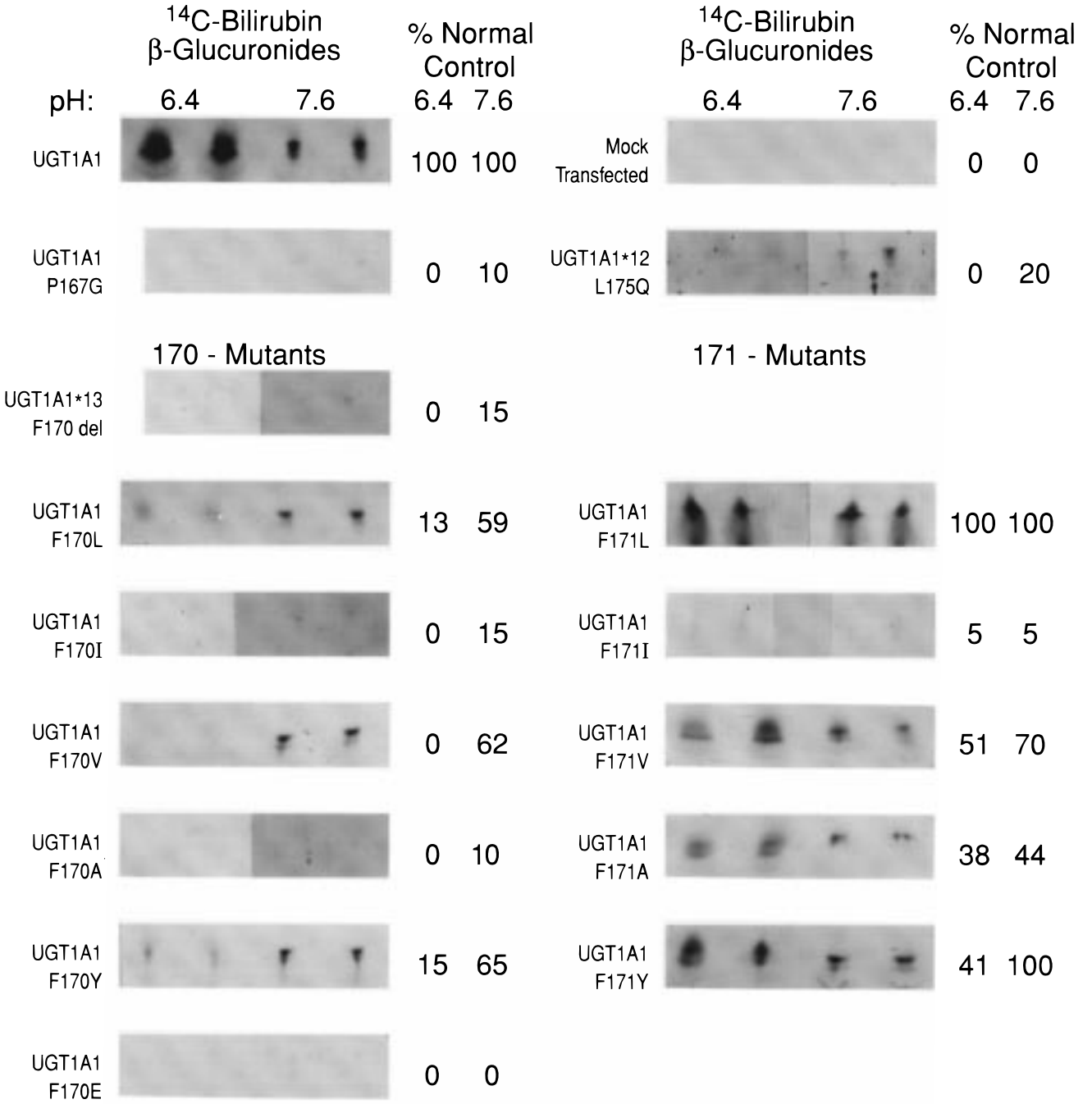

FIGURE 3: Bilirubin glucuronidation by the UGT1A1 (wild-type) and mutant UGT1A1 proteins measured at pH 6.4 and 7.6. Bilirubin glucuronidation was carried out using 1.41 mM [^{14}C]UDP-glucuronic acid (1.4 mCi/mmol) with either 20 mM sodium phosphate, pH 6.4, or 33 mM triethanolamine, pH 7.6. The reactions are described in detail in the Materials and Methods, contained from 0.3 to 0.6 mg of protein upon normalization, and incubated for 16 h at room temperature. The three ^{14}C bilirubin β-glucuronides comigrated and were separated in a TLC chromatography system as described in the Materials and Methods. The plates were exposed to X-ray film and developed to generate a glossy; the region containing the product in each case is shown.

the theory that these residues form an aromatic milieu capable of attracting bilirubin.

This highly conserved MRA with high hydrophobicity and aromaticity in the bilirubin-type transferase isozymes that is critical for catalysis was first uncovered between amino acid residues 159−177 upon finding a homozygous deleterious Phe-deletion mutation at position 170 of the isozyme from a CN-I patient (*8*). The comparisons made in this study demonstrate that this region of the bilirubin-type isoform is similar to that in the phenol-type transferases but show important differences with steroid-type isozymes as shown in Table 1. The Phe-170 residue is part of four consecutive residues with high hydrophobicity/aromaticity in the bilirubin-type isozymes; the phenol-metabolizing isoforms have a similar motif that differs marginally. A closer comparison shows a Phe-Phe, a Tyr-Phe, or Phe-Leu at the 170/171 position in the bilirubin-types, whereas the phenol-types show evidence for both less of a requirement for an aromatic residue in the 170 position or of consecutive aromatic residues. This strong aromatic/hydrophobic region between 169 and 172 appears to be disrupted by Ser in the steroid isoforms as shown in Table 1 (diagonal arrow).

For the first time, we probed for more detailed properties of the UDP-glucuronosyltransferase isozymes by using the

RAOARGOS program (*20, 21*) with algorithms based specifically on the properties of membrane-bound proteins. The demonstration in Figure 1 of a buried helix in the bilirubin- (UGT1A1) and the phenol (UGT1A6)-type enzymes centered over residues between 169 and 172 (or the equivalent position) with a positive value of 1.22 and 1.14, respectively, and the lack of one in the steroid-type (UGT2B7) isozymes appear to parallel the relative hydrophobic nature (water insolubilities) of the bilirubin, phenol, and steroid substrates, respectively. Notably, the amino acid sequence in this region of the steroid is altered in a manner that, among other changes, reduces hydrophobicity/aromaticity. This structure/site has the potential to discriminate between potential acceptor substrates based on hydrophobic binding/interaction(s).

The total loss of pH 6.4 activity by the mutant with the Gln-175 substituted for the hydrophobic Leu in the Crigler−Najjar Type I patient specified by the UGT1A1*13 allele further demonstrates a requirement for the hydrophobic character of this MRA region. We showed that the pH 6.4 activity was totally abolished with 20% of pH 7.6 activity remaining for this mutant. The RAOARGOS program (Table 1) predicts that the buried helix extends from residue 159 to 177 in the UGT1A1 protein supporting the requirement for a hydrophobic 175 residue. According to the program, this region extends from 152 to 175 in the UGT1A6 protein.

Our substitutions at the 170/171 position indicate that Phe-170 cannot be replaced. The nearly equally hydrophobic Leu had only 13/59% activity at pH 6.4/7.6, and the nearly equally aromatic, but less hydrophobic Tyr, had 15/65% normal activity at pH 6.4/7.6. The relatively conservative substitutions, Ile-170, Val-170, Ala-170, or the deletion of Phe-170 completely inactivated UGT1A1 at pH 6.4. All 170 alterations (Figure 3), except for Glu, showed that the pH 6.4 activity was more sensitive than that at pH 7.6. Glu-170 abolished all activity. Since neither a conservative hydrophobic alkyl nor aromatic residue completely restored activity, the results indicate that both the hydrophobicity and aromaticity of Phe-170 are obligated.

Phe-171, on the other hand, was replaced by Leu without any loss of activity. The progressively more hydrophobic residues, Ala-, Val-, and Leu-171, gave progressively more activity at both pH values such that Leu-171 exhibited activity comparable to the native protein. Compared with Tyr-170, activity with the Tyr-171 mutant increased from 15 to 44% and 65 to 100% of the wild-type activity at pH 6.4 and 7.6, respectively. Ile-171 was completely inactive, which suggests that the wild-type structure has a restricted conformation and efficient packing without steric clashes (*29*). The results demonstrate that while the Phe-170 is not replaceable, the Phe171 is completely replaceable by a nonaromatic, but highly hydrophobic residue. The fact that residue 171 was restricted to a substantially hydrophobic residue agrees with its location at the core of a buried structure (*29*).

Since the phenol-type UGT1A6 also contains a buried helix centered over the 170/171 position with the less hydrophobic, but aromatic Tyr-170 and the hydrophobic Leu-171, we questioned whether this isoform could in fact glucuronidate bilirubin. This protein glucuronidated bilirubin in vitro at a level 1/10 that of UGT1A1 and with a higher K_m value of 25 μM versus 5.0 μM (data not shown). Hence, the amino acid differences between the two isoforms cause a less efficient bilirubin-glucuronidating activity by the UGT1A6 isozyme. It should be pointed out that the UGT1A1 and UGT1A6 proteins are overall 67% similar in the unique amino terminus (286/535 residues) and are identical in the 246 carboxyl terminus as specified by the complex *UGT1* locus (*4*).

Although Gly substitution of the conserved Pro-167 was totally inactive, we showed in a previous study that Gly replacement of conserved Pro-285 had 39/74% normal activity at pH 6.4 and 7.6 (*30*). Bowie et al. (*29*) showed that a Pro, Phe, and Ile in an α-helical segment of the N-terminal domain of the λ repressor could not be replaced whereas all other amino acids in the 17 residue peptide are replaceable to varying extents.

Seppen et al. (*11*) measured activity for UGT1A1*12 at pH 7.8 and demonstrated some 60% activity remaining but with a 10-fold higher K_m value$_{Bilirubin}$ than normal. On the basis of 60% activity remaining, the authors concluded the patient was a moderately ill CN-II patient. Although the physiologically relevant activity, pH 6.4 and/or 7.6, is not known, the severe hyperbilirubinemia of the patient is consistent with a far greater loss of activity. The loss of the pH 6.4 activity, which is typically 2−4-fold higher than that at pH 7.6, could account for the severe CN-I phenotype. Since the hyperbilirubinemia of the patient might be expected to overcome the higher K_m (bilirubin) of the mutant enzyme, it is likely that the activity remaining in vivo is not as high as 60% for this allele.

Hence, the results from the CN-I patients and the amino acid substitution data at position 170/171 of the UGT1A1 isoform are evidence that the aromaticity/hydrophobicity in a buried helix structure is critical for bilirubin glucuronidation. A buried helix at the active site requiring certain hydrophobic protein−protein interactions, possibly with the membrane lipid bilayer, could explain the uniquely poor reconstitution of bilirubin transferase activity—compared to other isoforms—during purification conditions (*31*). Tertiary structures may undergo irreversibe alterations. Although the description of this hydrophobic and buried structure is, no doubt, incomplete, future studies concerning the active site and tertiary structure of the protein that modifies this highly hydrophobic-behaving compound will likely include this site.

REFERENCES

1. Roy Chowdhury, J., Wolkoff, A. W., Roy Chowdhury, N., and Arias, I. M. (1995) in *The Metabolic Basis of Inherited Disease* (Scriver, C. R., Beaudet, A. L., Sly, W. S., and Valle, D., Eds.) 7th ed., Vol. II, pp 2161−2208, McGraw-Hill Book Co., New York.
2. Ritter, J. K., Yeatman, M. T., Ferriera, P., and Owens, I. S. (1992) *J. Clin. Invest. 90*, 150−155.
3. Ritter, J. K., Crawford, J. M., and Owens, I. S. (1991) *J. Biol. Chem. 266*, 1043−1047.
4. Ritter, J. K., Chen, F., Sheen, Y. Y., Tran, H. M., Kimura S., Yeatman. M. T., and Owens, I. S. (1992) *J. Biol. Chem. 267*, 3257−3261.
5. Owens, I. S., and Ritter, J. K. (1995) *Prog. Nucl. Acid Res. Mol. Biol. 51*, 305−338.
6. Bosma, P. J., Roy Chowdhury, J., Huang, T-. J., Lahiri, P., Oude Elferink, R. P. J., Van Es, H. H. G., Lederstein, M., Whitington, P. F., Jansen, P L. M., and Roy Chowdhury, N. (1992) *FASEB J.* 6, 2859−2863.

7. Mackenzie, P. I., Owens, I. S., Burchell, B., Bock, K. W., et al. (1997) *Pharmacogenetics 7*, 255−269.
8. Ritter, J. K., Yeatman, M. T., Kaiser, C., Gridelli, B., and Owens, I. S. (1993) *J. Biol. Chem. 268*, 23573−23579.
9. Ciotti, M., Yeatman, M. T., Sokol, R. J., and Owens, I. S. (1995) *J. Biol. Chem. 270*, 3284−3291.
10. Ciotti, M., Marrone, A., Potter, C., and Owens, I. S. (1997) *Pharmacogenetics 7*, 585−595.
11. Seppen, J., Bosma, P. J., Goldhoorn, B. G., Bakker, C. T. M., Roy Chowdhury, J., Roy Chowdhury, N., Jansen, P. L. M., and Oude Elferink, R. P. J. (1994) *J. Clin. Invest. 94*, 2385−2391.
12. Ritter, J. K., Sheen, Y. Y., and Owens, I. S. (1990) *J. Biol. Chem. 265*, 7900−7906.
13. Bansal, S. K., and Gessner, T. (1980) *Anal. Biochem. 109*, 321−329.
14. Sato, H., Koiwai, O., Tanabe, K., and Kashiwamata, S. (1990) *Biochem. Biophys. Res. Commun. 169*, 260−264.
15. Kong, T. Ah-Ng, Ma, M., Tao, D., and Yang, L. (1993) *Pharm. Res. 10* (3), 461−465.
16. Philipp, T., Durazzo, M., Trautwein, C., Alex, B., Johnson, E. F., Straub, J. G. Straub, P., Tukey, R. H., and Manns, M., GenBank Accession no. 0CU09101.
17. Harding, D., Fournel-Gigleux, S., Jackson, M. R., and Burchell, B. (1988) *Proc. Natl. Acad. Sci. U.S.A. 85*, 8381−8385.
18. Iyanagi, T., Haniu, M., Sogawa, K., Fujii-Kuriyama, Y., Watanabe, S., Shively, J. E., and Anan, K. F. (1986) *J. Biol. Chem. 261*, 15607−15614.
19. Philipp, T., Durazzo, M., Trautwein, C., Alex, B., Straub, P., Lamb, J. G., Tukey, R. H., and Manns, M., GenBank Accession no. 0CU09030.
20. Mohana Rao, J. K. and Argos, P. (1986) *Biochim. Biophys. Acta 869*, 197−214.
21. Mohana Rao, J. K., Argos, P., and Hargrave, P. A. (1982) *Eur. J. Biochem. 128*, 565−575.
22. Chothia, C. (1976) *J. Mol. Biol. 105*, 1−14.
23. Bonnett, R., Davies, J. E., and Hursthouse, M. B. (1976) *Nature 262*, 326−328.
24. Blankaert, N., Heirwegh, K. P. M., and Zaman, Z. (1977) *Biochem. J. 164*, 229−236.
25. Listowsky, I. Gatmaitan, Z., and Arias, I. M. (1978) *Proc. Natl. Acad. Sci. 75*, 1213−1216.
26. Brown, J. R. (1978) in *Albumin, Structure, Biosynthesis, Function* (Peters, T., and Sjöholm, I., Eds.) FEBS 11th Meeting p 1, Pergamon Press, Oxford and Copenhagen.
27. Levi, A. J., Gatmaitan, Z., and Arias, I. M. (1969) *J. Clin. Invest. 48*, 2156−2167.
28. Brodersen, R. (1980) *CRC Crit. Rev. Clin. Lab. Sci. 11*, 304−399.
29. Bowie, J. U., Reidhaar-Olson, J. F. Lim, W. A., and Sauer, R. T. (1990) *Science 247*, 1306−1310.
30. Ciotti, M., and Owens, I. S. (1996) *Biochemistry 35*, 10119−10124.
31. Burchell, B. (1980) *FEBS Lett. 111*, 131−135.

BI980747Q